

# JGR Space Physics

## RESEARCH ARTICLE

10.1029/2024JA032576

### Key Points:

- With joint observations of THMIS-A and THMIS-E, we first report the prompt disappearance of chorus waves due to the high-speed jets (HSJs)
- HSJs cause the local indentation of the magnetopause, creating two new magnetic mirrors, and electrons are expelled by the mirror force
- The electron flux drop leads to the cessation of the chorus wave generation, that is, the disappearance of waves

### Supporting Information:

Supporting Information may be found in the online version of this article.

### Correspondence to:

X. Gao,  
[gaoxl@mail.ustc.edu.cn](mailto:gaoxl@mail.ustc.edu.cn)








### Citation:

Zhou, X., Gao, X., Lu, Q., Hajra, R., Ke, Y., Chen, R., & Ma, J. (2024). Prompt disappearance of magnetospheric chorus waves caused by high-speed magnetosheath jets. *Journal of Geophysical Research: Space Physics*, 129, e2024JA032576. <https://doi.org/10.1029/2024JA032576>

Received 23 FEB 2024

Accepted 3 JUN 2024

## Prompt Disappearance of Magnetospheric Chorus Waves Caused by High-Speed Magnetosheath Jets

Xuan Zhou<sup>1,2</sup> , Xinliang Gao<sup>1,2</sup> , Quanming Lu<sup>1,2</sup> , Rajkumar Hajra<sup>1,2</sup> , Yangguang Ke<sup>1,2</sup> , Rui Chen<sup>1,2</sup> , and Jiuqi Ma<sup>1,2</sup> 

<sup>1</sup>CAS Key Lab of Geospace Environment, School of Earth and Space Sciences, University of Science and Technology of China, Hefei, China, <sup>2</sup>CAS Center for Excellence in Comparative Planetology, Hefei, China

**Abstract** Magnetosheath high-speed jets (HSJs), localized impulses of dynamic pressure, are attracting growing attention due to their geoeffectiveness. However, how HSJs modulate chorus waves in the magnetosphere still remains unclear. Utilizing combined observations of the Time History of Events and Macroscale Interactions during Substorms satellites *A* and *E*, we report, for the first time, the prompt disappearance of the magnetospheric chorus waves caused by a HSJ. Such wave disappearance is directly due to the flux drop of energetic electrons ( $\sim 10$ – $100$  keV), leading to the cessation of wave generation, which is supported by the linear theoretical analysis. We propose that the flux drop results from the local indentation of magnetopause after the HSJ impact, where two new smaller magnetic mirrors are formed off the equator and part of electrons are then expelled by the mirror force. The HSJs should be an important factor in modulating chorus waves because of their high occurrence rate.

**Plain Language Summary** The solar wind with enhanced dynamic pressure can globally compress the dayside magnetosphere, causing the excitation and intensification of chorus waves. Besides the enhancement of solar wind RAM pressure, there also exists the ion-scale dynamic pressure impulse in the magnetosheath, known as a high-speed jet (HSJ), even during quiet solar wind conditions. Previous studies have shown that the HSJs have a high occurrence rate and they are geoeffective (causing disturbances in the Earth's magnetosphere). However, it is still unknown whether HSJs can modulate chorus waves in the magnetosphere. In this study, based on joint observations of THEMIS-A and E probes, we report the prompt disappearance of chorus waves in the magnetosphere caused by the HSJs. We propose that a HSJ causes the local indentation of the dayside geomagnetic fields at the magnetic equator, and creates two small magnetic mirrors. Consequently, the poleward mirror force will expel some of the electrons from the equator, and lead to a significant decrease of the electron flux. Finally, the generation of chorus waves will stop due to the lack of energy sources. This study reveals that HSJs are a new and important factor in modulating chorus waves in the magnetosphere.

## 1. Introduction

Whistler-mode chorus waves are right-hand polarized electromagnetic emissions frequently detected in the Earth's magnetosphere (Tsurutani & Smith, 1974). They are excited by several to tens of keV anisotropic electrons due to cyclotron resonant instabilities (Tsurutani et al., 1979) in the frequency range of  $0.1$ – $0.5f_{ce}$  (lower band) and  $0.5$ – $0.8f_{ce}$  (upper band), separated by  $0.5f_{ce}$  (Burtis & Helliwell, 1976; Gao et al., 2019; Tsurutani & Smith, 1974). Here  $f_{ce}$  denotes the equatorial electron gyrofrequency. Because the chorus waves can cause both significant loss (Gao et al., 2023; Thorne et al., 2005, 2010; Tsurutani et al., 2013) and acceleration (Horne et al., 2005; Li et al., 2016; Thorne et al., 2013) of electrons by the resonant scattering, they are known to play a crucial role in the dynamics of the Earth's radiation belts.

Satellite observations have shown that chorus waves are sensitive to changes in the solar wind RAM pressure. In general, solar wind with enhanced dynamic pressure compresses the dayside magnetosphere, leading to the betatron acceleration of electrons and the reduction of the geomagnetic field inhomogeneity, which are favorable for the excitation and intensification of chorus waves (Fu et al., 2012; Jin et al., 2022; Ma et al., 2022; Remya et al., 2015; Yue et al., 2017; X. Y. Zhou & Tsurutani, 1999; C. Zhou et al., 2015; X. Zhou et al., 2023).

Besides the enhancement of solar wind RAM pressure, there also exist ion-scale dynamic pressure impulses in the Earth's subsolar magnetosheath. These impulses, characterized by high-speed and dense plasma flows, are named as high-speed jets (HSJs) (Hietala & Plaschke, 2013). The formation of HSJs is probably associated with the

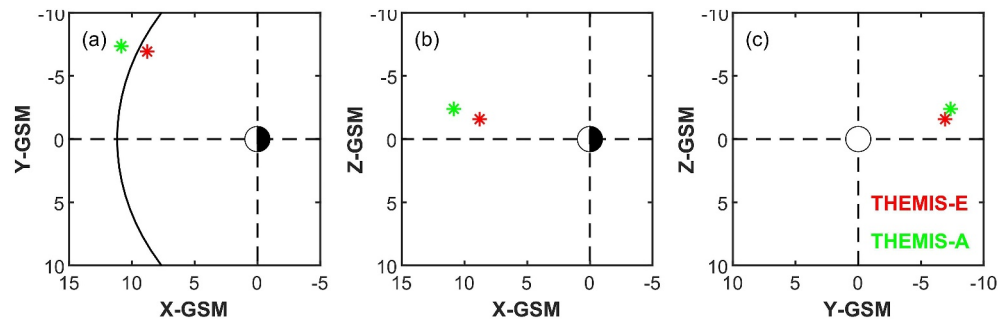


**Figure 1.** The position of THEMIS-A (green mark) and THEMIS-E (red mark) in the x-y (a), x-z (b), and y-z (c) planes in the geocentric solar magnetospheric coordinate system at 10:25 UT on 8 August 2016, respectively.

interaction between the compressive structures upstream of the quasi-parallel bow shock and the shock front (Guo et al., 2022; Hao et al., 2016; Hietala et al., 2009; Karlsson et al., 2015; Ren et al., 2023). Unlike a global-scale compression of the dayside magnetosphere by a solar wind RAM pressure, a HSJ only locally compresses the dayside magnetosphere due to its smaller scale size ( $\sim 1 R_E$  parallel to the propagation direction, and a few  $R_E$  perpendicular to the propagation direction;  $R_E$  is the Earth radius) (Archer et al., 2012; Dmitriev & Suvorova, 2012, 2015; Hietala et al., 2012; Plaschke et al., 2016; Shue et al., 2009). Such local impact can cause large amplitude boundary indentations, possibly triggering dayside magnetic reconnection (Hietala et al., 2018), exciting ULF waves in the magnetosphere (Wang et al., 2018, 2022), and resulting in dayside fast flow channels in the ionosphere (Hietala et al., 2012), and localized auroral brightenings (Wang et al., 2018). However, till date, it is unknown whether HSJs can modulate chorus waves in the Earth's magnetosphere.

In this paper, utilizing the joint observations from the Time History of Events and Macroscale Interactions during Substorms satellites A (THMIS-A) and E (THMIS-E), we report the prompt disappearance of chorus waves in the magnetosphere caused by a magnetosheath HSJ for the first time. The unexpected disappearance of chorus waves is directly related to a fast drop of the energetic electron fluxes, which resulted from a local indentation of the geomagnetic field after the HSJ hits the magnetopause. In Section 2, we briefly describe the instruments onboard THEMIS. The joint observations are demonstrated in Section 3. Finally, we summarize and discuss the principal results in Section 4.

## 2. Instruments and Data

The THEMIS spacecraft, launched on 17 February 2007, consists of five identical satellites (A-E) in near-equatorial orbits. With apogees above  $10 R_E$  and perigees below  $2 R_E$ , THEMIS provides a good opportunity for the multi-site detection of plasma environments in the Earth's magnetosheath and magnetosphere. A fluxgate magnetometer (FGM) onboard THEMIS records background magnetic fields. A search-coil magnetometer (SCM) and an electric field instrument (EFI) record tri-axial magnetic and electric fields with a sampling rate of up to  $\sim 8$  kHz, respectively. An electrostatic analyzer (ESA) provides the pitch-angle distribution of electrons with energies from a few eV to 30 keV, and solid state telescopes (SST) provide that for 30 keV to  $\sim 1$  MeV electrons. The electron density is inferred from the spacecraft potential measured by EFI and thermal velocity measured by ESA.

## 3. Observational Results

The joint observations of THEMIS-A and THEMIS-E at 10:25 UT on 8 August 2016 are utilized in this study due to their favorable locations. Figure 1 shows the locations of THEMIS-A (green) and THEMIS-E (red) in the geocentric solar magnetospheric (GSM) coordinate system. The black line in Figure 1a indicates the position of magnetopause on the x-y plane according to Shue et al. (1998) model. Both THEMIS-A and THEMIS-E are located in the pre-noon sector (magnetic local time (MLT)  $\sim 9.5$  hr) near the magnetic equator. They are  $\sim 2 R_E$  apart in the X-direction and less than  $1 R_E$  apart in the Y- and Z-directions. Fortunately, THEMIS-A was located in the magnetosheath during this time, while THEMIS-E was operating in the magnetosphere.

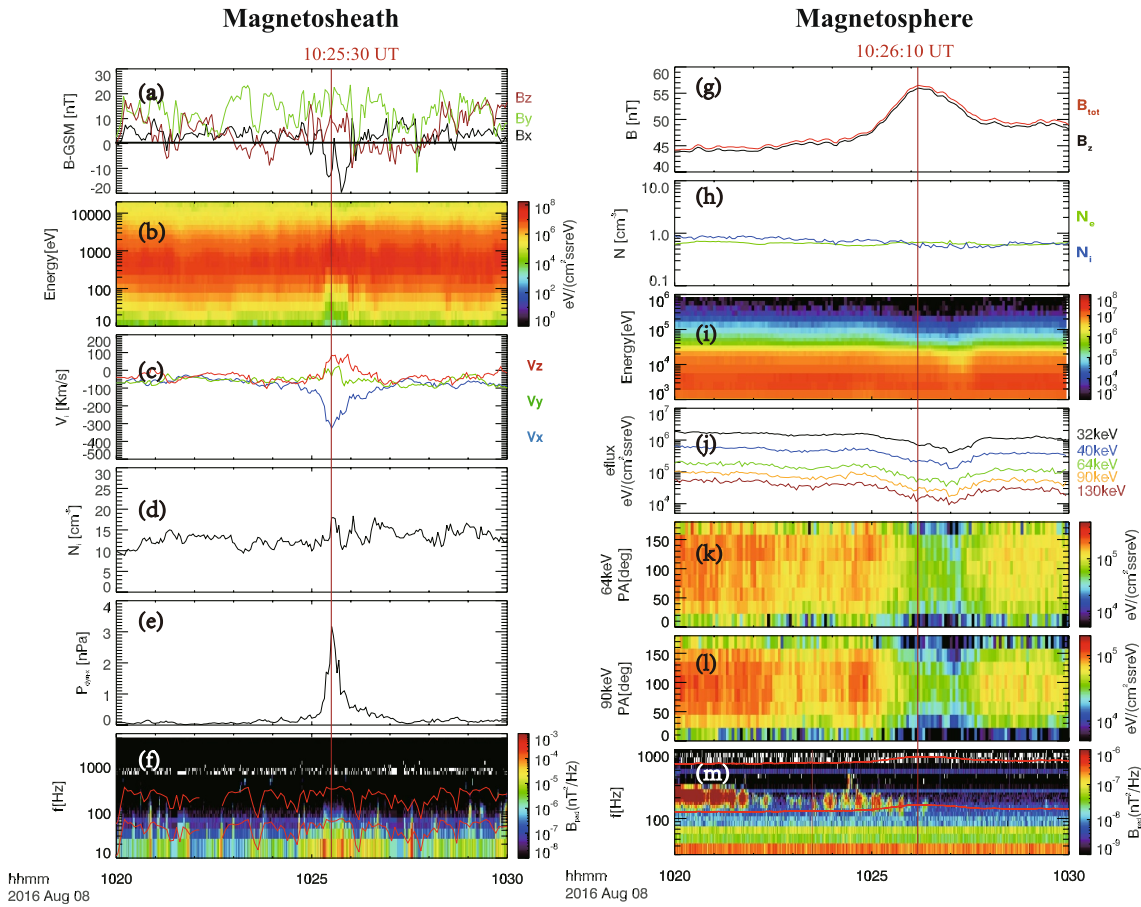


**Figure 2.** The overview of a high-speed jet in the magnetosheath observed by THEMIS-A from 10:20 to 10:30 UT on 8 August 2016 (a–e), and the response in the magnetosphere detected by TH-E during the same period (f–l). (a) The magnetic field in the geocentric solar magnetospheric (GSM) coordinate system, (b) ion energy flux, (c) ion velocity in the GSM coordinate system, (d) ion density, (e) the dynamic pressure ( $P_{\text{dynx}}$ ) in the  $X$ -direction, (f) magnetic power spectral densities ( $B_{\text{psd}}$ ) in magnetosheath, (g) the geomagnetic field in magnetosphere ( $B_{\text{tot}}$ , red line) and its  $Z$ -direction component ( $B_z$ , black line), (h) background electron density and ion density, (i) electron energy flux, (j) electron energy flux for 32, 41, 65, 93, 139 keV, (k–m) electron pitch angle distributions for 65 and 93 keV, (l) magnetic power spectral densities ( $B_{\text{psd}}$ ) in magnetosphere. The two red lines in (f) and (l) represent  $0.05 f_{\text{ce}}$  and  $0.5 f_{\text{ce}}$ .

Figure 2a–2f present the magnetosheath magnetic field and plasma measurements by THEMIS-A from 10:20 to 10:30 UT on 8 August 2016. The turbulent background magnetic fields are distributed from several nT to 20 nT (Figure 2a), and ions have energies ranging from a few eV to tens of keV (Figure 2b), consistent with the typical plasma environment in the Earth's magnetosheath (Lucek et al., 2005). Figures 2c–2e illustrate the bulk velocity, density, and dynamic pressure  $x$ -component ( $P_{\text{dynx}}$ ) of ions, respectively. Around 10:25 UT, there is a sudden enhancement of ion velocity and density, leading to the  $P_{\text{dynx}}$  pulse ( $\sim 3.2$  nPa), which is identified as a HSJ in the magnetosheath (marked by a red vertical line). The  $P_{\text{dynx}}$  pulse is accompanied by a series of intense waves (Figure 2f). We cannot determine if these waves are magnetosheath lion roars (Smith and Tsurutain, 1976), because the polarization cannot be determined due to the lack of burst-mode data. More effort is needed to identify the waves accompanied with HSJs, which is beyond scope of the present work. During this time interval, the solar wind RAM pressure is  $\sim 1.5$  nPa, and the interplanetary magnetic field remains northward (not shown), suggesting a relatively quiet solar wind condition.

Figures 2g–2m display the magnetosphere response, as detected by THEMIS-E, to the HSJ. Slightly later than the  $P_{\text{dynx}}$  pulse in the magnetosheath, the geomagnetic field shows a clear compression signal, that is,  $B_z$  (black line) and  $B_{\text{tot}}$  (red line) simultaneously increased by  $\sim 11$  nT (Figure 2g). In this event, the HSJ mainly propagates in the  $X$ -direction ( $v_x \sim 330$  km  $s^{-1}$ , Figure 2c), and the positions of THEMIS-A and THEMIS-E are mainly separated in the  $X$ -direction ( $\Delta d \sim 2 R_E$ ). We estimate a  $\sim 38$  s travel time of the HSJ by dividing the distance between two satellites by the speed of the HSJ in the  $X$ -direction. This is roughly consistent with the time delay ( $\sim 40$  s) between

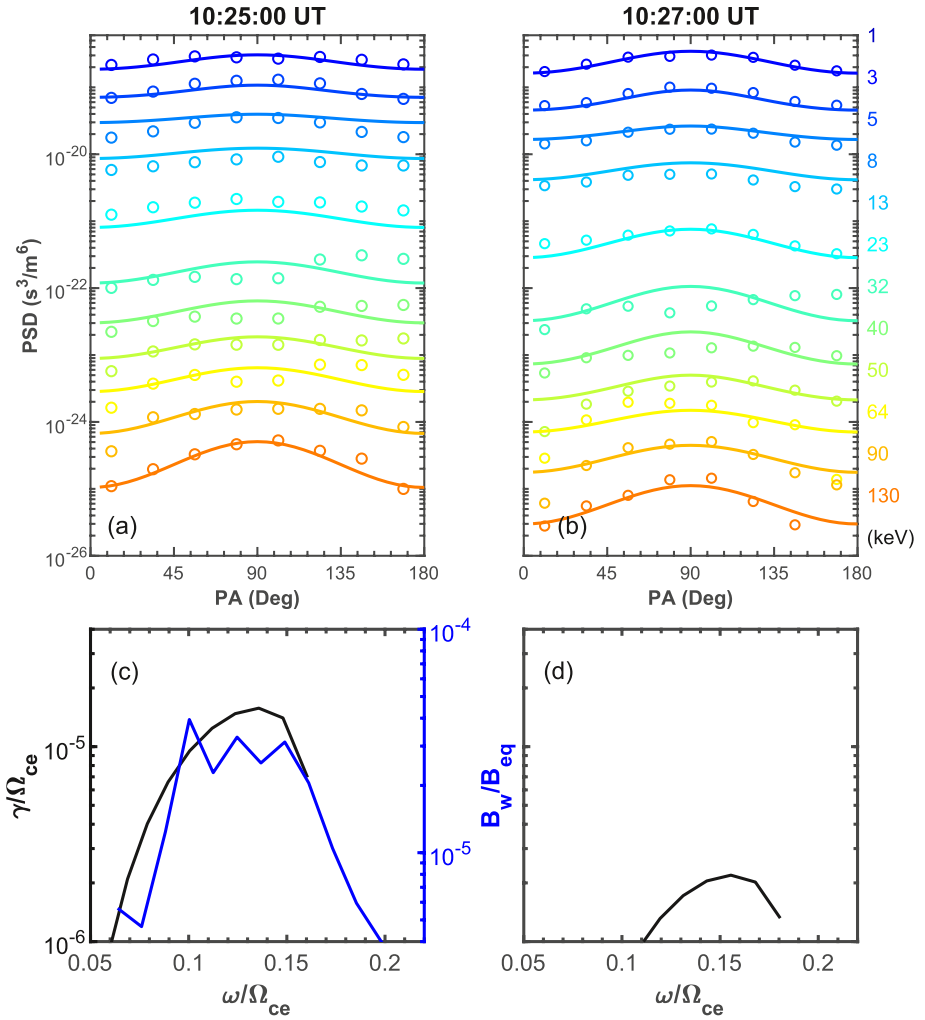


**Figure 3.** (a–b) Observed (circles) and fitted (lines) electron phase space densities before and after the compression of geomagnetic field, (c) linear growth rates (black) and the wave amplitudes (blue) before the compression of geomagnetic field, (d) linear growth rates after the compression of geomagnetic field.

the HSJ and the geomagnetic field compression. Therefore, it is reasonable to conclude that the geomagnetic local compression is caused by the HSJ impact. In addition, the background plasma density nearly remains constant during this period (Figure 2h). Figure 2i shows the evolution of fluxes of electrons with energies from several keV to hundreds of keV, and Figure 2j shows the evolution for five selected energies. Unexpectedly, the compression of geomagnetic fields is accompanied by a remarkable decline of energetic electron ( $\sim 10$ – $100$  keV) flux. The pitch-angle distributions of 65 and 93 keV electrons are presented in Figures 2k and 2l, showing that the electron fluxes drop at nearly all pitch angles. Figure 2m displays the magnetic power spectral densities ( $B_{psd}$ ) during this period. The typical chorus waves can be clearly observed before the compression of geomagnetic fields. However, the waves suddenly disappear as the geomagnetic field strength increases.

We propose that the disappearance of the chorus waves is a direct response to the electron flux drop. Figures 3a and 3b present the pitch-angle distributions (circles) of electrons before and after the local geomagnetic field compression, respectively. The observed distribution is fitted to a multi-component bi-Maxwellian distribution function:

$$f_M(v_{\parallel}, v_{\perp}) = \sum_j \sqrt{\frac{m}{2T_{\parallel j}\pi}} \frac{m}{2T_{\perp j}\pi} n_j e^{-\frac{m v_{\parallel}^2}{2T_{\parallel j}} - \frac{m v_{\perp}^2}{2T_{\perp j}}}, \quad (1)$$

**Table 1**  
Fitting Parameters Before (10:25:00 UT) and After (10:27:00 UT) the Compression of the Geomagnetic Field, Respectively

Component ( <i>j</i> )	10:25:00 UT			10:27:00 UT		
	$T_{\parallel}$ (eV)	$T_{\perp}$ (eV)	$n$ (cm <sup>-3</sup> )	$T_{\parallel}$ (eV)	$T_{\perp}$ (eV)	$n$ (cm <sup>-3</sup> )
1	100	100	0.4	100	100	0.4
2	900	1,200	0.1	800	1,100	0.15
3	4,000	4,500	0.07	3,600	4,300	0.045
4	8,000	9,000	0.002	8,000	9,000	0.0005
5	22,000	30,000	0.0002	22,000	30,000	0.000045

where the  $m, n_j, T_{\parallel j}$ , and  $T_{\perp j}$  are the electron mass, electron density, electron parallel temperature, and electron perpendicular temperature for the  $j$  th component, respectively. The fitted distributions (solid lines) are shown in Figures 3a and 3b, and the fitting parameters are listed in Table 1. Comparison of observations with the fitting results shows a good consistency. Furthermore, we use a dispersion relation solver (BO) (Xie, 2019) to search for the unstable plasma waves by the fitting parameters, and the calculated linear growth rates of chorus waves are illustrated in Figures 3c and 3d (black). The normalized amplitude (blue line) of chorus waves is also plotted in Figure 3c. Before the geomagnetic field compression (Figure 3c), the frequency profile of the linear growth rates is consistent with that of wave amplitudes, supporting the local excitation of those waves by energetic electrons. However, after the compression (Figure 3d), the linear growth rate decreases by about

an order of magnitude, implying that the generation of chorus waves has been switched off. As a result, THEMIS-E did not observe any chorus waves near the magnetic equator. Here we should mention that the enhancement of geomagnetic fields has only a weak effect on the wave disappearance, since the linear growth rate will change slightly if we artificially fix the electron distribution.

Figure 4 shows the distribution functions of the 10–100s keV electrons before (green) and after (orange) the compression of geomagnetic field. The flux drop of energetic electrons caused by the HSJ should be an adiabatic process, since the distribution functions of 10–100s keV electrons before and after the local compression of geomagnetic fields have the same shape. However, how does a HSJ cause the adiabatic modulation of electron flux? In Figure 5, we schematically show the response of the dayside magnetosphere to a HSJ. Before the arrival of the HSJ, the dayside magnetosphere exhibits a dipole-like configuration, which acts as a large magnetic mirror to trap a population of energetic electrons (Figure 5a). The electrons bounce along the field lines between the south and north mirror points, and are unstable to excite chorus waves at the equator due to their temperature anisotropy. After the arrival of the HSJ, the magnetopause is heavily compressed at the location (c) where the HSJ hits, leading to a local indentation on the outer field lines at the magnetic equator (Figure 5b). The local indentation causes a local maximum of magnetic field intensity at the equator, which further leads to the formation of two small magnetic mirrors. As a result, a part of the electrons with larger pitch angles are expelled by the mirror force, and now bounce between the south (north) mirror point and the new equatorial mirror point. A part of electrons with smaller pitch angles still able to pass the equatorial region, they now have a larger pitch angle. Therefore, THEMIS-E detected the remarkable flux drop of energetic electrons, as well as the disappearance of chorus waves inside the magnetosphere.

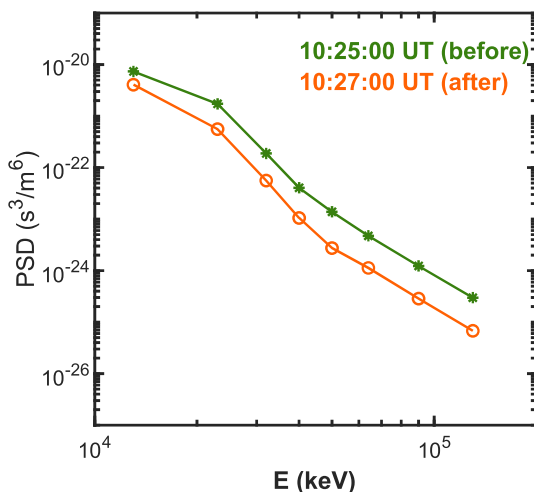


**Figure 4.** The distribution functions of the 10–100s keV electrons before (green) and after (orange) the compression of geomagnetic field.

#### 4. Discussion and Conclusions

Utilizing the joint observations of THEMIS-A and THEMIS-E, we, for the first time, report the disappearance of chorus waves in the magnetosphere caused by a magnetosheath HSJ. The HSJ is firstly captured by THEMIS-A in the magnetosheath, and then it impacts on the dayside magnetosphere after ~40 s. THEMIS-E, flying in the magnetosphere, observed the sudden flux drop of energetic electrons (~10–100 keV), as well as a prompt disappearance of chorus waves as impacts of the HSJ. We propose that a HSJ impinging on the magnetopause will create two new small magnetic mirrors near the magnetic equator due to the local indentation of the geomagnetic fields. As a result, a part of the electrons will be expelled from the equator by the mirror force, causing the electron flux drop at the equator. Such an electron flux drop leads to the cessation of wave generation, or the disappearance of chorus waves. We have also presented another event detected by THEMIS-A and THEMIS-E during 21:00–21:10 UT on 24 June 2016 in Figures 6 and 7. We find a similar situation that the chorus waves promptly disappear after the HSJ hits the Earth's magnetosphere, implying that the disappearance of chorus waves caused by HSJs may be a common phenomenon.



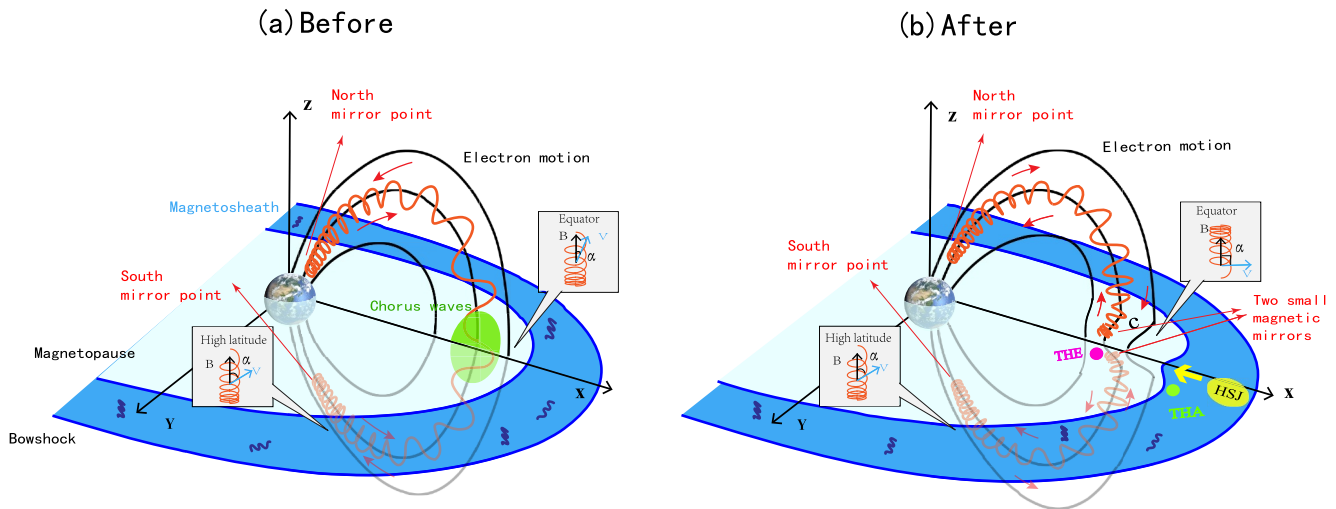


**Figure 5.** Schematic diagram of the magnetosheath and magnetosphere in the geocentric solar magnetospheric (GSM) coordinate system before (a) and after (b) the hit of high-speed jet. The configuration of the geomagnetic field is based on TS04 model (Tsyganenko & Sitnov, 2005), and the positions of TH-A and TH-E in the GSM coordinate system are marked by a green point and a plum red point (b), respectively. The small diagrams (gray) provide a variation in the electron pitch angle as it moves along the magnetic field line.

Both a HSJ and an enhanced solar wind RAM pressure can compress the dayside magnetosphere, but the response of the magnetospheric chorus is different. This is due to the different spatial scales of the compression of Earth's dayside magnetic field caused by the two processes, which is shown schematically in Figure S1 (in Supporting Information S1). The solar wind RAM pressure can compress the magnetic field on a global scale (Figure S1b), resulting in a flatter but stronger magnetic field and a betatron acceleration of electrons. Consequently, chorus waves are more easily generated, and preferentially occur in a wide range of magnetic latitudes on the dayside (Ma et al., 2022). However, HSJs only cause the local indentation of Earth's dayside magnetic field due to its small scale size (Figure S1c). The local indentation causes a local maximum of magnetic field intensity near the equator, and leads to the formation of two small magnetic mirrors (Figure S1c). Now, a part of the electrons that move toward the equator will be expelled by the magnetic mirror force and trapped in the higher latitudes, and the electrons originally at the equator will leave the equator. Therefore, the electron flux at the equator rapidly drops, leading to the cessation of wave generation. Note that these disappeared electrons near the equator are now trapped at high latitudes, and they will not precipitate into the atmosphere and cause auroral brightenings. Since HSJs are frequently observed in the magnetosheath (Plaschke et al., 2016), we propose that HSJs are a new and important factor in modulating chorus waves in the magnetosphere.

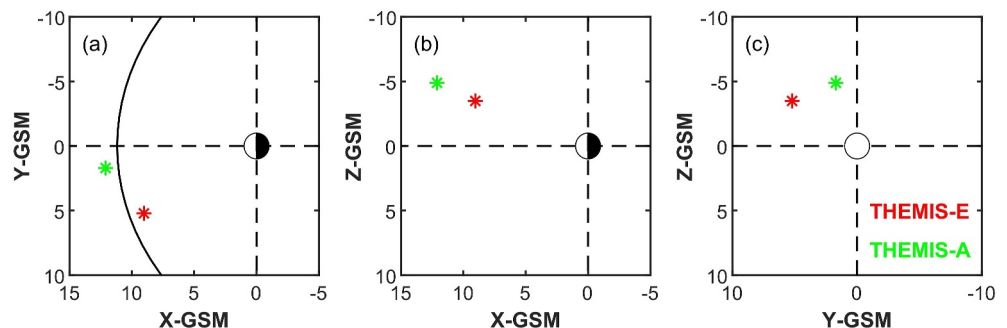


**Figure 6.** The position of THEMIS-A (green mark) and THEMIS-E (red mark) in the x-y (a), x-z (b), and y-z (c) planes in the geocentric solar magnetospheric coordinate system for another event at 21:04 UT on 26 June 2016, respectively.

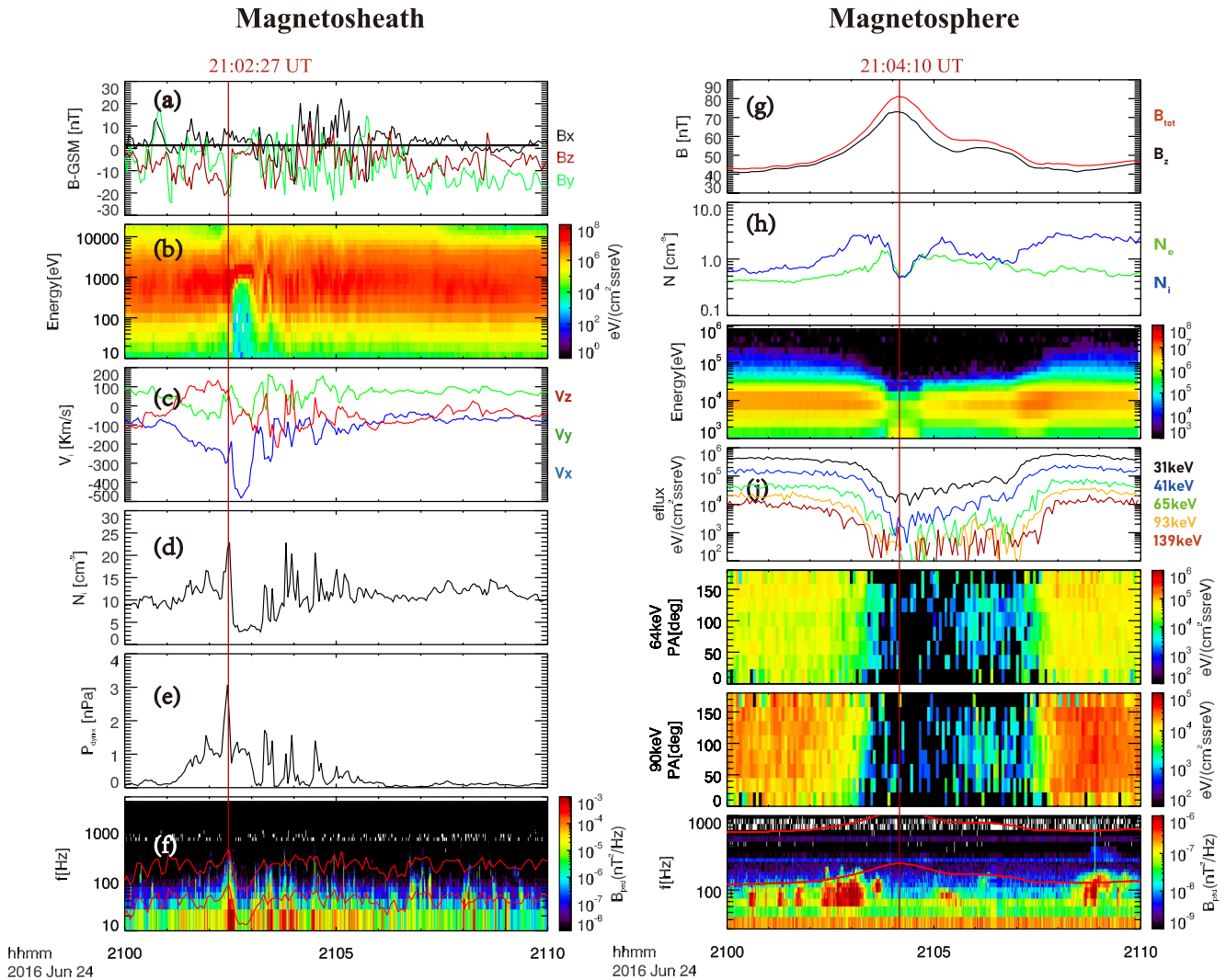


**Figure 7.** The overview of a high-speed jet in magnetosheath observed by THEMIS-A from 21:00 to 21:10 UT on 24 Jun 2016 (a–f), and the response in magnetosphere detected by THEMIS-E during the same period (g–m) in the same format as Figure 2.

### Data Availability Statement

The THEMIS data used in this study are obtained from the website <http://themis.ssl.berkeley.edu/data/themis>. The OMNI data are obtained from the website <http://spdf.gsfc.nasa.gov/pub/data/omni/>.

### Acknowledgments

This research was funded by the NSFC Grant 42322406 and 42230201, Strategic Priority Research Program of Chinese Academy of Sciences Grant XDB41000000, Fundamental Research Funds for the Central Universities (KY208000063), and “USTC Tang Scholar” program. We also acknowledge the entire THEMIS instrument group.

### References

- Archer, M. O., Horbury, T. S., & Eastwood, J. P. (2012). Magnetosheath pressure pulses: Generation downstream of the bow shock from solar wind discontinuities. *Journal of Geophysical Research*, *117*(A5), A05228. <https://doi.org/10.1029/2011JA017468>
- Burtis, W. J., & Helliwell, R. A. (1976). Magnetospheric chorus: Occurrence patterns and normalized frequency. *Planetary and Space Science*, *24*(11), 1007–1024. [https://doi.org/10.1016/0032-0633\(76\)90119-7](https://doi.org/10.1016/0032-0633(76)90119-7)
- Dmitriev, A. V., & Suvorova, A. V. (2012). Traveling magnetopause distortion related to a large-scale magnetosheath plasma jet: THEMIS and ground-based observations. *Journal of Geophysical Research*, *117*(A8), A08217. <https://doi.org/10.1029/2011JA016861>
- Dmitriev, A. V., & Suvorova, A. V. (2015). Large-scale jets in the magnetosheath and plasma penetration across the magnetopause: THEMIS observations. *Journal of Geophysical Research*, *120*(6), 4423–4437. <https://doi.org/10.1002/2014JA020953>
- Fu, H. S., Cao, J. B., Mozer, F. S., Lu, H. Y., & Yang, B. (2012). Chorus intensification in response to interplanetary shock. *Journal of Geophysical Research*, *117*(A1), A01203. <https://doi.org/10.1029/2011JA016913>
- Gao, X., Chen, L., Li, W., Lu, Q., & Wang, S. (2019). Statistical results of the power gap between lower-band and upper-band chorus waves. *Geophysical Research Letters*, *46*(8), 4098–4105. <https://doi.org/10.1029/2019GL082140>
- Gao, X., Ma, J., Shao, T., Chen, R., Ke, Y., & Lu, Q. (2023). Why chorus waves are the dominant driver for diffuse auroral precipitation. *Science Bulletin*, *ISSN*, *69*(5), 2095–2273. <https://doi.org/10.1016/j.scib.2023.12.009>

- Guo, J., Lu, S., Lu, Q., Lin, Y., Wang, X., Ren, J., et al. (2022). Large-scale high-speed jets in Earth's magnetosheath: Global hybrid simulations. *Journal of Geophysical Research*, *127*(6), e2022JA030477. <https://doi.org/10.1029/2022JA030477>
- Hao, Y., Lembege, B., Lu, Q., & Guo, F. (2016). Formation of downstream high-speed jets by a rippled nonstationary quasi-parallel shock: 2-D hybrid simulations. *Journal of Geophysical Research*, *121*(3), 2080–2094. <https://doi.org/10.1002/2015JA021419>
- Hietala, H., Laitinen, T. V., Andréová, K., Vainio, R., Vaivads, A., Palmroth, M., et al. (2009). Supermagnetosonic jets behind a collisionless quasiparallel shock. *Physical Review Letters*, *103*(24), 245001. <https://doi.org/10.1103/physrevlett.103.245001>
- Hietala, H., Partamies, N., Laitinen, T. V., Clausen, L. B. N., Facskó, G., Vaivads, A., et al. (2012). Supermagnetosonic subsolar magnetosheath jets and their effects: From the solar wind to the ionospheric convection. *Annals of Geophysics*, *30*(1), 33–48. <https://doi.org/10.5194/angeo-30-33-2012>
- Hietala, H., Phan, T. D., Angelopoulos, V., Oieroset, M., Archer, M. O., Karlsson, T., & Plaschke, F. (2018). In situ observations of a magnetosheath high-speed jet triggering magnetopause reconnection. *Geophysical Research Letters*, *45*(4), 1732–1740. <https://doi.org/10.1002/2017GL076525>
- Hietala, H., & Plaschke, F. (2013). On the generation of magnetosheath high-speed jets by bow shock ripples. *Journal of Geophysical Research*, *118*(11), 7237–7245. <https://doi.org/10.1002/2013JA019172>
- Horne, R., Thorne, R., Shprits, Y., Meredith, N. P., Glauert, S. A., Smith, A. J., et al. (2005). Wave acceleration of electrons in the Van Allen radiation belts. *Nature*, *437*(7056), 227–230. <https://doi.org/10.1038/nature03939>
- Jin, Y., Liu, N., Su, Z., Zheng, H., Wang, Y., & Wang, S. (2022). Immediate impact of solar wind dynamic pressure pulses on whistler-mode chorus waves in the inner magnetosphere. *Geophysical Research Letters*, *49*(5), e2022GL097941. <https://doi.org/10.1029/2022GL097941>
- Karlsson, T., Kullen, A., Liljeblad, E., Brenning, N., Nilsson, H., Gunell, H., & Hamrin, M. (2015). On the origin of magnetosheath plas-moids and their relation to magnetosheath jets. *Journal of Geophysical Research: Space Physics*, *120*(9), 7390–7403. <https://doi.org/10.1002/2015JA021487>
- Li, W., Ma, Q., Thorne, R. M., Bortnik, J., Zhang, X. J., Li, J., et al. (2016). Radiation belt electron acceleration during the 17 March 2015 geomagnetic storm: Observations and simulations. *Journal of Geophysical Research*, *121*(6), 5520–5536. <https://doi.org/10.1002/2016JA022400>
- Lucek, E. A., Constantinescu, D., Goldstein, M. L., Pickett, J., Pinçon, J. L., Sahraoui, F., et al. (2005). The magnetosheath. *Space Science Reviews*, *118*(1–4), 95–152. <https://doi.org/10.1007/s11214-005-3825-2>
- Ma, J., Gao, X., Chen, H., Tsurutani, B. T., Ke, Y., Chen, R., & Lu, Q. (2022). The effects of substorm injection of energetic electrons and enhanced solar wind ram pressure on whistler-mode chorus waves: A statistical study. *Journal of Geophysical Research*, *127*(11), e2022JA030502. <https://doi.org/10.1029/2022JA030502>
- Plaschke, F., Hietala, H., Angelopoulos, V., & Nakamura, R. (2016). Geoeffective jets impacting the magnetopause are very common. *Journal of Geophysical Research*, *121*(4), 3240–3253. <https://doi.org/10.1002/2016JA022534>
- Remya, B., Tsurutani, B. T., Reddy, R. V., Lakhina, G. S., & Hajra, R. (2015). Electromagnetic cyclotron waves in the dayside subsolar outer magnetosphere generated by enhanced solar wind pressure: EMIC wave coherency. *Journal of Geophysical Research*, *120*(9), 7536–7551. <https://doi.org/10.1002/2015JA021327>
- Ren, J., Lu, Q., Guo, J., Gao, X., Lu, S., Wang, S., & Wang, R. (2023). Two-dimensional hybrid simulations of high-speed jets downstream of quasi-parallel shocks. *Journal of Geophysical Research*, *128*(8), e2023JA031699. <https://doi.org/10.1029/2023JA031699>
- Shue, J.-H., Chao, J.-K., Song, P., McFadden, J. P., Suvorova, A., Angelopoulos, V., et al. (2009). Anomalous magnetosheath flows and distorted subsolar magnetopause for radial interplanetary magnetic fields. *Geophysical Research Letters*, *36*(18), L18112. <https://doi.org/10.1029/2009GL039842>
- Shue, J.-H., Song, P., Russell, C. T., Steinberg, J. T., Chao, J. K., Zastenker, G., et al. (1998). Magnetopause location under extreme solar wind conditions. *Journal of Geophysical Research*, *103*(A8), 17691–17700. <https://doi.org/10.1029/98JA01103>
- Smith, E. J., & Tsurutani, B. T. (1976). Magnetosheath lion roars. *Journal of Geophysical Research*, *81*(13), 2261–2266. <https://doi.org/10.1029/JA081i013p02261>
- Thorne, R., Li, W., Ni, B., Ma, Q., Bortnik, J., Chen, L., et al. (2013). Rapid local acceleration of relativistic radiation-belt electrons by magnetospheric chorus. *Nature*, *504*(7480), 411–414. <https://doi.org/10.1038/nature12889>
- Thorne, R., Ni, B., Tao, X., & Meredith, N. P. (2010). Scattering by chorus waves as the dominant cause of diffuse auroral precipitation. *Nature*, *467*(7318), 943–946. <https://doi.org/10.1038/nature09467>
- Thorne, R. M., O'Brien, T. P., Shprits, Y. Y., Summers, D., & Horne, R. B. (2005). Timescale for MeV electron microburst loss during geomagnetic storms. *Journal of Geophysical Research*, *110*(A9), A09202. <https://doi.org/10.1029/2004JA010882>
- Tsurutani, B. T., Lakhina, G. S., & Verkhoglyadova, O. P. (2013). Energetic electron (>10 keV) microburst precipitation, similar to 5–15 s X-ray pulsations, chorus, and wave-particle interactions: A review. *Journal of Geophysical Research: Space Physics*, *118*(5), 2296–2312. <https://doi.org/10.1002/jgra.50264>
- Tsurutani, B. T., & Smith, E. J. (1974). Postmidnight chorus: A substorm phenomenon. *Journal of Geophysical Research*, *79*(1), 118–127. <https://doi.org/10.1029/JA079i001p0118>
- Tsurutani, B. T., Smith, E. J., West Jr, H. I., & Buck, R. M. (1979). Chorus, energetic electrons and magnetospheric substorms. In P. J. Palmadesso & K. Papadopoulos (Eds.), *Wave instabilities in space plasmas* (Vol. 71, pp. 55–62). D. Reidel. <https://doi.org/10.1007/978-94-009-9500-06>
- Tsyganenko, N. A., & Sitnov, M. I. (2005). Modeling the dynamics of the inner magnetosphere during strong geomagnetic storms. *Journal of Geophysical Research*, *110*(A3), A03208. <https://doi.org/10.1029/2004JA010798>
- Wang, B., Nishimura, Y., Hietala, H., & Angelopoulos, V. (2022). Investigating the role of magnetosheath high-speed jets in triggering dayside ground magnetic ultra-low frequency waves. *Geophysical Research Letters*, *49*(22), e2022GL099768. <https://doi.org/10.1029/2022GL099768>
- Wang, B., Nishimura, Y., Hietala, H., Lyons, L., Angelopoulos, V., Plaschke, F., et al. (2018). Impacts of magnetosheath high-speed jets on the magnetosphere and ionosphere measured by optical imaging and satellite observations. *Journal of Geophysical Research*, *123*(6), 4879–4894. <https://doi.org/10.1029/2017JA024954>
- Xie, H. (2019). BO: A unified tool for plasma waves and instabilities analysis. *Computer Physics Communications*, *244*, 343–371. <https://doi.org/10.1016/j.cpc.2019.06.014>
- Yue, C. C., Bortnik, J. L., Ma, Q., Thorne, R. M., Angelopoulos, V., Spence, H. E., et al. (2017). The characteristic response of whistler mode waves to interplanetary shocks. *Journal of Geophysical Research*, *122*(10), 10047–10057. <https://doi.org/10.1002/2017JA024574>
- Zhou, C., Li, W., Thorne, R. M., Bortnik, J., Ma, Q., An, X., et al. (2015). Excitation of dayside chorus waves due to magnetic field line compression in response to interplanetary shocks. *Journal of Geophysical Research*, *120*(10), 8327–8338. <https://doi.org/10.1002/2015JA021530>



- Zhou, X., Gao, X., Chen, R., Lu, Q., Ke, Y., Ma, J., & Kong, Z. (2023). Direct observation of rising-tone chorus triggered by enhanced solar wind pressure. *Journal of Geophysical Research*, *128*(11), e2023JA031787. <https://doi.org/10.1029/2023JA031787>
- Zhou, X., & Tsurutani, B. T. (1999). Rapid intensification and propagation of the dayside aurora: Large scale interplanetary pressure pulses (fast shocks). *Geophysical Research Letters*, *26*(8), 1097–1100. <https://doi.org/10.1029/1999GL900173>